

Causal inference for disruption management in urban metro networks

Nan Zhang^a

nan.zhang16@imperial.ac.uk

Daniel Hörcher^a

d.horcher@imperial.ac.uk

Prateek Bansal^b

prateekb@nus.edu.sg

Daniel J. Graham^{a*}

d.j.graham@imperial.ac.uk

^a Transport Strategy Centre, Department of Civil and Environmental Engineering, Imperial College London, London, UK

^b Department of Civil and Environmental Engineering, National University of Singapore, Singapore

* Corresponding author

Abstract

Urban metro systems can provide highly efficient and effective movements of vast passenger volumes in cities, but they are often affected by disruptions, causing delays, crowding, and ultimately a decline in passenger satisfaction and patronage. To manage and mitigate such adverse consequences, metro operators could benefit greatly from a quantitative understanding of the causal impact of disruptions. Such information would allow them to predict future delays, prepare effective recovery plans, and develop real-time information systems for passengers on trip re-routing options. In this paper, we develop a performance evaluation tool for metro operators that can quantify the causal effects of service disruptions on passenger flows, journey times, travel speeds and crowding densities. Our modelling framework is simple to implement, robust to statistical sources of bias, and can be used with high-frequency large-scale smart card data (over 4.85 million daily trips in our case) and train movement data. We recover disruption effects at the points of disruption (e.g. at disrupted stations) as well as spillover effects that propagate throughout the metro network. This allows us to deliver novel insights on the spatio-temporal propagation of delays in densely used urban public transport networks. We find robust empirical evidence that the causal impacts of disruptions adversely affect service quality throughout the network, in ways that would be hard to predict absent a causal model.

Key words: Sustainable transport, Metro disruption, Impact propagation, Causal inference

1. Introduction

Commitment to a carbon neutral future presents enormous challenges for patterns of consumption, production, and energy use. Changes in the transport sector will play a key role in achieving net zero emissions, requiring more sustainable movements including a shift in passenger transport away from private car. Sustainable transport choices are better incentivised when alternatives to private car are efficient, reliable, and resilient. Metro systems form an important component of mass public transport in cities, characterised by large capacity and high-frequency services that can deliver vast volumes of passengers to central locations in small windows of time. However, metros experience disruptions frequently due to infrastructure or rolling stock failure, extreme demand shocks, bad weather or natural disasters, leading to a decline in service quality and ultimately in attractiveness and patronage (Zhang et al., 2016). To manage and respond to disruptions, operators' recovery strategies require detailed information about the number of travellers affected, delay times, and the crowding density inside trains and on platforms across the metro network. This information provides the foundation for prediction and management of future interruptions, and for the provision of real-time information that can mitigate the impact of disruptions on passengers.

In the literature, a large number of simulation studies have been conducted to quantify the impacts of hypothetical disruption scenarios. Over the years, these simulation-based research has evolved from solely using complex network theory to encompassing system-performance analysis (Derrible and Kennedy, 2010; Mattsson and Jenelius, 2015; Sun et al., 2015; Sun and Guan, 2016; Malandri et al., 2018; Yap and Cats, 2022). However, the absence of real disruption data and user responses raises doubts about the validity of the assumptions made regarding virtual interruptions and the corresponding passenger behaviour. In contrast, empirical studies have adopted observational data, such as passenger surveys and smart card data, to analyse the effects of disruptions (Rubin et al., 2005; Silva et al., 2015; Sun et al., 2016; Zhu et al., 2017; Yap and Cats, 2020; Zhang et al., 2021). Most existing empirical research typically assumes that metro disruptions occur randomly. However, it is crucial to acknowledge that some internal or external factors may have a significant confounding influence on the likelihood of metro failures, as well as the corresponding impact of disruptions, which needs to be considered in the quantification (Melo et al., 2011; Zhang et al., 2021). Moreover, metro stations are interconnected through an infrastructure network, which implies that disruption impacts can propagate from any point to the entire network. This interference problem is challenging to address even using state-of-art intervention evaluation methods.

To address the above gaps, we propose a novel causal inference framework to quantify both the direct and spillover causal effects of metro disruptions on system performances, which is characterised by passenger demand, average travel speed/journey time, and on-board crowding level. Our synthetic control method is unique in the way that it allows interference among metro stations, and the weighted average of unaffected observations (synthetic control) is used to approximate the counterfactual outcomes of disruptions. Specifically, the multi-day high-frequency smart card data (over 4.85 million trips per weekday) enable us to create a control group for each metro station across the disrupted day using data observed on days when disruptions did not happen in the entire metro network. Thus, the proposed approach estimates the network-wide impact of disruptions by relaxing the non-interference assumption and eliminating any potential confounding bias.

We conducted a case study of four urban lines of the Hong Kong Mass Transit Railway (MTR) and illustrated it with a randomly selected disruption on the Island Line. This application indicates that delays and crowding can spread throughout the entire disrupted line and potentially affect other lines within the network. The propagation of spillover effects takes time and the disrupted station may recover earlier than other parts of the network, with impacts on downstream stations lagging behind that on upstream stations. Additionally, we find that interchange stations, those with connections to more than two metro lines, are more resistant to disturbance from disruptions, especially for journey time, travel speed and crowding density. The above unbiased information offers important insights for metro operators, enabling them to improve the quality of real-time information provision and replacement service planning during disruptions. The success of this case study also demonstrates that our causal framework is easy to use, scalable, and can be extended to other complex transportation systems for intervention assessment and operational decisions.

The rest of the paper is organised as follows. Section 2 reviews the literature on quantifying the effects of metro disruptions, with a focus on empirical research. Section 3 presents the proposed synthetic control framework. This section outlines the fundamentals of Rubin’s potential outcome framework and the customised synthetic control design to estimate the disruption impact across a metro network by leveraging high-frequency smart card data. In Section 4, we detail the case study on the Hong Kong MTR with an example of network-level disruption impacts propagation. Finally, results and conclusions are discussed in Section 5 and Section 6.

2. Literature review

There are various ways in which we can model and quantify the impacts of metro disruptions. The literature is rich in simulation studies of various interruption scenarios. Simulations enable the measurement of the impact of disruptions on network accessibility, vulnerability, and resilience. Traditional simulation-based analyses rely on complex network theory, which converts the metro network into a scale-free graph (Derrible and Kennedy, 2010; Mattsson and Jenelius, 2015). By hypothetically removing nodes or links, measures such as location importance, betweenness centrality and global efficiency are derived to reflect the changes in the topological structure of the metro network under disruption (Sun et al., 2015; Yang et al., 2015; Sun and Guan, 2016; Sun et al., 2018; Zhang et al., 2018). More advanced simulation-based research also incorporates metro operations into impact estimation (Mattsson and Jenelius, 2015). Via passenger-route assignment, disruption impacts are often quantified as the variance in ridership distribution, passenger delays, operational costs, or crowding level under different hypothetical scenarios (Sun et al., 2018; Rodríguez-Núñez and García-Palomares, 2014; Cats and Jenelius, 2014; Malandri et al., 2018; Adjetey-Bahun et al., 2016; M’cleod et al., 2017; Yap et al., 2022). The simulation approach can imitate a wider range of situations through the experimental settings, from station closures to network crashes (Sun et al., 2015; Sun and Guan, 2016; Zhang et al., 2018; Chopra et al., 2016; Zhang et al., 2018; Ye and Kim, 2019). However, in general many assumptions have to be made to infer passengers’ responses to virtual disruptions. Without observing passengers’ behaviour during real incidents, the veracity of the simulation approach is largely questionable (Zhang et al., 2021).

Due to the abovementioned concerns, empirical studies have gained popularity with the availability of a variety of data sources, from user surveys (Rubin et al., 2005; Zhu et al., 2017) to automated smart

card data (Silva et al., 2015; Sun et al., 2016; Yap and Cats, 2020; Zhang et al., 2021). The latter has emerged as the mainstream data source in recent years due to their advantages in terms of accuracy, cost-effectiveness, and ease of long-term observation (Sun et al., 2013; Kusakabe and Asakura, 2014). For example, Sun et al. (2016) applied smart card data to estimate the disruption impact as the difference in passenger assignment outcomes under real incidents and normal conditions. Silva et al. (2015) estimated the loss of demand at entry and exit stations under disruptions from smart card data and the topology of the metro network.

The above-discussed empirical literature typically assumes that metro disruptions occur randomly. However, factors such as the underlying travel patterns, the type of signalling, passenger behaviour, the condition and age of the infrastructure and rolling stock, and weather conditions may have a significant confounding influence on the likelihood of metro failures, as well as the corresponding impact of disruptions, hindering our ability to truly measure cause and effect patterns of disruption (Melo et al., 2011; Wan et al., 2015; Brazil et al., 2017). Zhang et al. (2021) relaxed the random disruption assumption and proposed a propensity score matching method to quantify average causal disruption effects that addresses potential bias from confounding factors. The design of their causal inference method still suffers from the limitation that it cannot capture the spillover effects of disruptions on nearby metro stations (also known as the “interference” phenomenon). Metro stations are connected by an infrastructure network and served sequentially by trains, meaning that disruption impacts can propagate from any point to the entire network. This shortcoming is challenging to address using traditional causal inference methods.

This research contributes to the literature by leveraging large-scale smart card data and historical disruption data to develop a novel statistical method which advances the field in two ways. First, adoption of a causal perspective renders our empirical approach free from confounding bias which would otherwise arise in naïve statistical analyses due to the non-random nature of disruption occurrence. Second, our causal inference framework enables operators to measure network spillover effects, following the pattern of delay propagation throughout the entire system. To the best of our knowledge, this is the first study that provide empirical evidence of the spillover disruption impacts and their spatio-temporal propagation.

3. Methodology

To measure the impact of disruptions on a metro system, we use Rubin’s potential outcome framework to establish causality (Rubin, 1974). We define metro disruptions as ‘treatments’ (or interventions) and the objective of our analysis is to quantify the direct and indirect causal effect of treatments on ‘outcomes’ related to the quality of service provision. Specifically, we are interested in estimating station-level impacts on (i) travel demand, (ii) journey times, (iii) travel speed of passengers, and (iv) crowding density on board. The detailed definition of each outcome measure is provided in the Appendix.

3.1 Synthetic control framework

In this research, we define the study unit as the status of a metro station $a = 1, \dots, A$ on a given day $d = 1, \dots, D$, during interval $t = 1, \dots, T$. We consider 15-minute-long intervals. The station is classed as *treated* if it encounters a service interruption of at least five minutes in the 15-minute interval. The

treatment assignment variable, denoted by $W_{adt} \in \{0,1\}$, records whether station a has been exposed to disruptions during interval t on day d . Under the assumption that there are no hidden versions of the treatment (consistency assumption), see (Imbens and Rubin; 2015), we use $Y_{adt}(W_{adt})$ to denote the potential outcomes of metro service provision, namely the total inflow and outflow of passengers, the average journey time, average travel speed, and the density of crowding. More specifically,

$$Y_{adt}(W_{adt}) = Y_{adt}(0) \times (1 - W_{adt}) + Y_{adt}(1) \times W_{adt}, \quad [1]$$

$$Y_{adt} = \begin{cases} Y_{adt}(0) & \text{if } W_{adt} = 0 \\ Y_{adt}(1) & \text{if } W_{adt} = 1, \end{cases}$$

where $Y_{adt}(0)$ and $Y_{adt}(1)$ are counterfactual potential outcomes, only one of which is observed. Causal inference studies commonly make the stable unit treatment value assumption (SUTVA), which requires that the outcome for each unit should be independent of the treatment status of other units (Graham et al., 2014). However, due to interference between stations in the metro network, SUTVA is unlikely to hold. We customize the synthetic control method to estimate causal effects of disruptions in the absence of SUTVA.

To create the synthetic counterfactual outcome, we create a donor pool from data observed on days when disruptions did not happen in the entire metro network: \mathbf{d}_N is a set of such undisrupted days with cardinality J . This design of the donor pool benefits from the fact that high-frequency smart card data contain observations for all time intervals from multiple days. To quantify the impact of a disruption that starts at station a_I on day d_I at time T_{IS} and ends at time T_{IE} , we construct a vector of outcomes $\mathbf{p} = \{\mathbf{p}_1, \mathbf{p}_2, \dots, \mathbf{p}_A\}$, where \mathbf{p}_a is the two-dimensional vector of outcomes for station a during time intervals $t = T_{IS}, \dots, T$ on the disrupted day d_I and J undisrupted days (i.e., $J + 1$ days). We assume that this disruption has no effect on outcomes before the treatment period T_{IS} . Conversely, after T_{IS} , all stations in the network can be affected by this disruption. Since we stack the data of the treated day followed by undisrupted days, $p_{ajt} = Y_{adt}(W_{adt})$ for $j = 1$ and $p_{ajt} = Y_{adjt}(W_{adjt})$ for $j = 2, \dots, J + 1$, $d_j \in \mathbf{d}_N$. Note that $W_{adt} = 1$ if $t \geq T_{IS}$ and $W_{adt} = 0$ otherwise.

For a specific time interval of a treated/affected station a , the counterfactual outcome is defined as a weighted average of the outcomes in the donor pool, where $\mathbf{C}^a = (c_2^a, \dots, c_{J+1}^a)'$ is a $J \times 1$ vector of non-negative weights that sum to one (Abadie, 2021). See the next subsection for the way we determine these weights. The synthetic control estimator of the counterfactual outcomes is:

$$\hat{Y}_{adt}^N = \sum_{j=2}^{J+1} c_j^a \cdot Y_{adjt}(0) \quad t = T_{IS}, \dots, T, \quad [2]$$

while the causal effect of the treatment is estimated by

$$\hat{\tau}_{adt} = Y_{adt} - \hat{Y}_{adt}^N \quad t = T_{IS}, \dots, T. \quad [3]$$

With the definitions above, during and after a given disruption, the direct causal effects on a treated station a_I is derived as

$$\tau_{a_I d_I t} = Y_{a_I d_I t}(1) - \sum_{j=2}^{J+1} c_j^{a_I} \cdot Y_{a_I d_j t}(0) \quad t = T_{IS}, \dots, T. \quad [4]$$

where $Y_{a_I d_I t}$ denotes the observed outcome of the treated unit on the disrupted day in interval t . Furthermore, $c_j^{a_I}$ denotes the weight of the j^{th} day in the corresponding donor pool for station a_I , and $Y_{a_I d_j t}(0)$ denotes the observed outcomes for the same station-interval pair on the j^{th} day.

Similarly, the indirect causal spillover effects of a disruption at station a_I on the performance of other station a_O ($a_O \in 1, \dots, A \setminus a_I$) is derived as

$$\tau_{a_O d_I t} = Y_{a_O d_I t}(1) - \sum_{j=2}^{J+1} c_j^{a_O} \cdot Y_{a_O d_j t}(0) \quad t = T_{IS}, \dots, T, \quad [5]$$

where $Y_{a_O d_I t}(1)$ denotes the observed outcomes for the affected units of other (non-disrupted) stations during and after a given disruption; $c_j^{a_O}$ and $Y_{a_O d_j t}(0)$ denote the weight and outcomes of the j^{th} day in the corresponding donor pool for station a_O . Figure 1 illustrates the design of the synthetic control framework for metro disruptions.

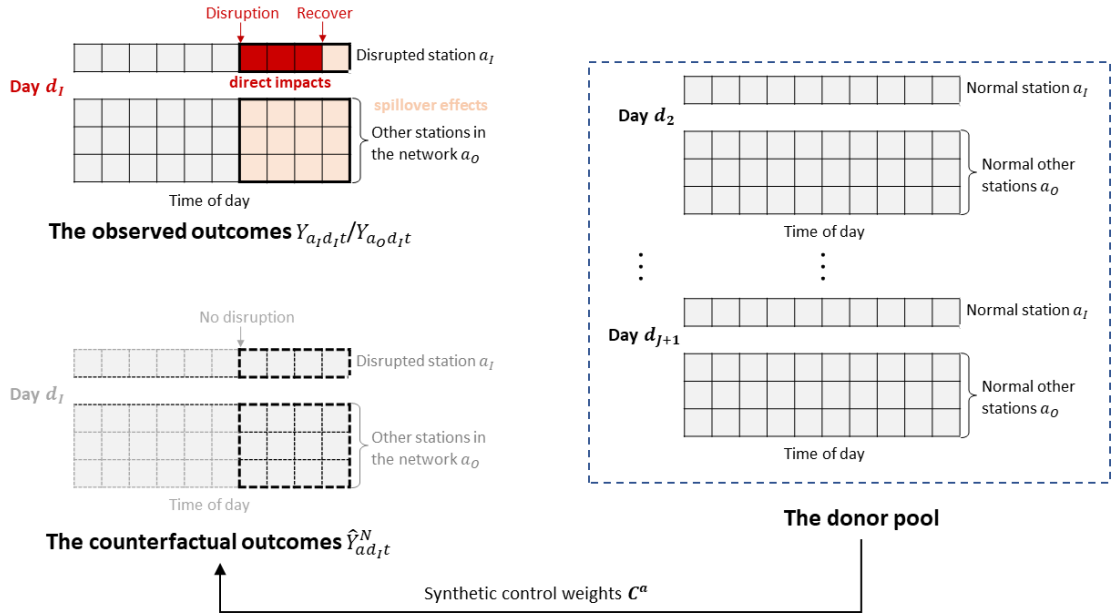


Figure 1. Schematic overview of the customised synthetic control method for metro disruptions. The donor pool consists of observations from non-disrupted days, and a_O represents any other undisrupted station in the network.

3.2 The choice of weights

A simple way of constructing synthetic counterfactuals is to assign equal weights $c_j^a = 1/J$ to each unit in the donor pool. The estimator for $\tau_{a d_I t}$ is then

$$\hat{\tau}_{a d_I t} = Y_{a d_I t} - \frac{1}{J} \sum_{j=2}^{J+1} Y_{a d_j t} \quad t = T_{IS}, \dots, T, \quad [6]$$

where the synthetic control is the unweighted average of observed historic outcomes in the donor pool.

In this research, we apply the method proposed by Abadie and Gardeazabal (2003) and Abadie et al. (2010) to determine C^a . For the disrupted day d_I and each day in the donor pool d_j corresponding to station a at time $t < T_{IS}$, we first collect data on a set of k predictors of the outcomes, denoted by $k \times 1$

vectors $\mathbf{X}_1^{at}, \mathbf{X}_2^{at}, \dots, \mathbf{X}_{J+1}^{at}$. Let $\mathbf{X}_1^a = \left(\frac{\sum_{t \in T_0} \mathbf{X}_{11}^{at}}{|T_0|}, \dots, \frac{\sum_{t \in T_0} \mathbf{X}_{1k}^{at}}{|T_0|} \right)$ be a $k \times 1$ vector and collect the values of such predictors at the disrupted day for a pre-intervention period $T_0 \subseteq \{1, 2, \dots, T_{IS} - 1\}$. Similarly, the $k \times J$ matrix $\mathbf{X}_0^a = [\mathbf{X}_2^a, \dots, \mathbf{X}_{J+1}^a]$ represents the predictors for the J non-disrupted days within this donor pool. Predictors \mathbf{X} are selected such that they are unaffected by the treatment (service interruption), but they do influence the outcomes, which may include pre-interruption values of Y_{adt} .

Weights \mathbf{C}^a are optimised to ensure that the resulting synthetic control units best resemble all relevant characteristics (predictors) of the treated unit before the disruption. That is, given a set of non-negative constants $\mathbf{V}^a = (v_1^a, \dots, v_k^a)$, the optimal synthetic control weight vector $\mathbf{C}^{a*} = (c_2^{a*}, \dots, c_{J+1}^{a*})'$ is obtained from the following minimisation problem:

$$\min_{\mathbf{C}^a} \|\mathbf{X}_1^a - \mathbf{X}_0^a \cdot \mathbf{C}^a\|_{\mathbf{V}^a} = \frac{1}{|T_0|} \sqrt{\sum_{h=1}^k v_h^a \cdot \sum_{t \in T_0} (X_{1h}^{at} - c_2^a \cdot X_{2h}^{at} - \dots - c_{J+1}^a \cdot X_{(J+1)h}^{at})^2},$$

such that $\sum_{j=2}^{J+1} c_j^a = 1, c_j^a > 0,$ [7]

where the positive constants v_1^a, \dots, v_k^a reflect the relative importance of the k predictors on the outcomes. Each potential choice of \mathbf{V}^a produces a corresponding set of synthetic control weights $\mathbf{C}(\mathbf{V}^a) = (c_2^a(\mathbf{V}^a), \dots, c_{J+1}^a(\mathbf{V}^a))'$. We choose \mathbf{V}^a , such that $\mathbf{C}(\mathbf{V}^a)$ minimises the mean squared prediction error (MSPE) of this synthetic control with respect to outcome Y_{adt}^N before the disruption:

$$\min_{\mathbf{V}^a} \sum_{t \in T_0'} \left(Y_{adt} - c_2^a(\mathbf{V}^a) \cdot Y_{ad_2t} - \dots - c_{J+1}^a(\mathbf{V}^a) \cdot Y_{ad_{J+1}t} \right)^2,$$

such that $\sum_{h=1}^k v_h^a = 1, v_h^a > 0,$ [8]

where the synthetic control weights $c_2^a(\mathbf{V}^a), \dots, c_{J+1}^a(\mathbf{V}^a)$ are functions of \mathbf{V}^a , for a pre-intervention period $T_0' \subseteq \{1, 2, \dots, T_{IS} - 1\}, T_0' \neq T_0$.

To determine the optimal values of \mathbf{V}^a and \mathbf{C}^a , we follow Abadie (2021) and the steps below.

- i). Divide the pre-intervention periods (before disruption occurs) into an initial training period ($t = 1, \dots, t_0$) and a subsequent validation period ($t = t_0 + 1, \dots, T_{IS} - 1$). The lengths of the training and validation periods can be application specific.
- ii). With training period data on the predictors, compute the synthetic control weights under given constants $\tilde{\mathbf{C}}^a(\mathbf{V}^a)$ by solving the optimisation problem in Equation [7].
- iii). Using data from the validation period, minimise the MSPE in Equation [8] with respect to \mathbf{V}^a .
- iv). With the validation period data on the predictors, use the resulting \mathbf{V}^{a*} to calculate optimal weights $\tilde{\mathbf{C}}^{a*} = \tilde{\mathbf{C}}^a(\mathbf{V}^{a*})$, according to Equation [7].

4. The Case study

Our case study application is based on large-scale automated data from four urban lines of Hong Kong MTR, the Island Line, Tsuen Wan Line, Kwun Tong Line and Tseung Kwan O Line, with 49 stations in total. A map of the partial network that we study is provided in Figure 2. The daily service hours of the four lines start at 6:00 and end at 24:00, which is then divided into 72 intervals of 15 minutes. The following data are used to estimate the direct and spillover causal effects of disruptions.

Pseudonymised smart card data: The Hong Kong MTR provided smart card data from 01/01/2019 to 31/03/2019. The dataset contains information on the time and location of tap-in and tap-out transactions throughout the system, recording individual trips. Based on the data, we compute aggregate passenger flows at station entries and exits, passenger's average journey time, the average travel speed (Zhang et al., 2021), and crowding density (Hörcher et al., 2017) for each target station. The resolution of time stamps exacts to one second.

Automated vehicle location (AVL) data and incidents logs: The MTR provided AVL data and incident information data during the same study period, which are used to generate historical disruption logs (Zhang et al., 2022). The AVL data contain information on train ID, service ID, the timestamp of train movements (including precise departure and arrival times), and the location of train movements (including station, line and directions). The resolution of time stamps exacts to one second. Incident logs are manual inspection record of incidents, including information on the time and location, cause and duration of disruptions. Readers are referred to Appendix for more details on our disruption data.

Weather data: We collect data on outside temperature, wind speed and precipitation status from the web portal Weather Underground of Hong Kong. Based on hourly historical observations, we estimate weather conditions for all selected stations at 15-minute intervals.

Mega events in Hong Kong: From 01/2019 to 03/2019, we collect information, including the location and time, on three types of mega-events held in Hong Kong: concerts, sports matches and exhibitions. Data sources include official news and government records.¹

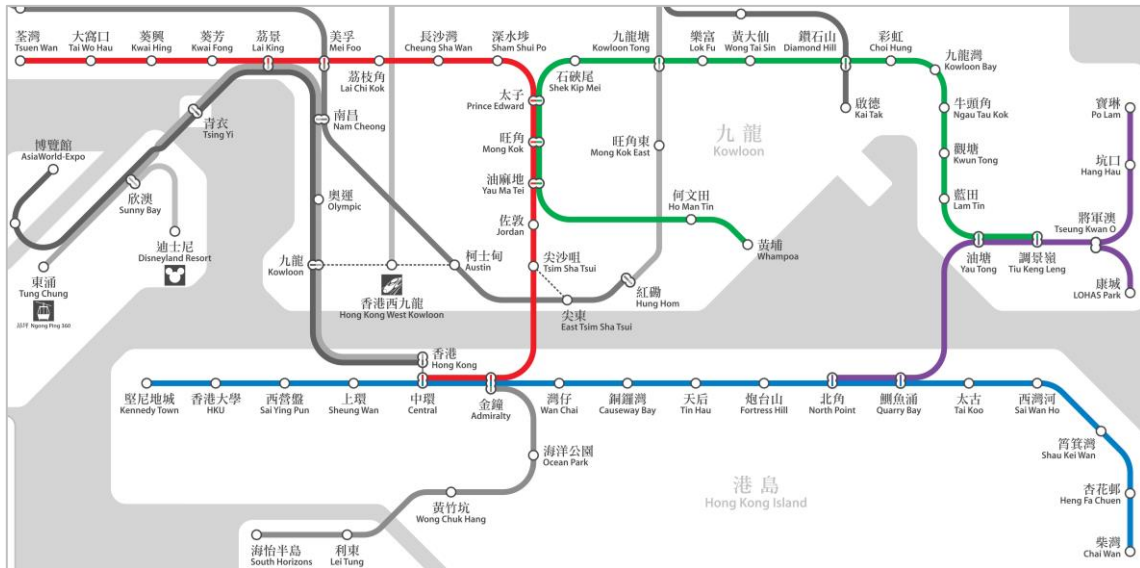


Figure 2. The map of four urban lines that we study in the MTR network (highlighted in colour).

¹ <https://www.mevents.org.hk/en/index.php>.

https://www.lcsd.gov.hk/tc/programmes/programmeslist/mqme_prog.html.

5. Results

Our study period runs from 1/1/2019 to 31/3/2019, and our analysis of data from Hong Kong MTR covers 54 weekdays, excluding holidays and a day when data from few lines are missing. The results of the case study are presented through a randomly selected disruption which occurred during the evening peak hours at Chai Wan station, the Eastern terminus of the Island Line, and lasted for 27 minutes.

5.1 Synthetic control design

The time of a service day is divided into 72 intervals of 15 minutes each, and the metro station in each 15-minute interval (station-interval) is our study unit. On Monday 11/3/2019, the selected disruption occurred at 17:41 and ended at 18:08. Thus, Chai Wan station was interrupted (treated) during this period (time interval: 47 to 48),² while the other 48 stations on the four urban lines were still functioning normally. Note that within the entire network, no other disruption occurred on the same day.³ Under the proposed framework, a treated station-interval is compared to a synthetic control unit that we generate from the “donor pool”, that is, historic observations from the same station in the same time interval, but on different days. In this study, 13 weekdays with no disruption are used to construct the donor pool.

We use the untreated and unaffected units from the donor pool to construct a “synthetic” control unit, of which the characteristics approximate that of the treated unit. The counterfactual outcome of the treatment is estimated by the untreated outcome of the synthetic control unit. We create a synthetic control unit by weighting historic observations of the same station-interval pair from undisrupted days. The weights are set to maximise the synthetic control’s ability to replicate observed exogenous characteristics (predictors) and metro service outcomes in the immediate pre-intervention time intervals at the treated station.

To account for the non-randomness of disruption occurrence, we consider partial confounding factors of metro disruptions when selecting predictors. These are summarised in Table 1. We divide 46 pre-intervention intervals into a training period (first 23 intervals) and a subsequent validation period (last 23 intervals), and construct the synthetic control in a three-stage iterative process (Abadie and Gardeazabal, 2003; Abadie et al., 2010). First, we optimise the set weights in the donor pool (as functions of given positive constants) to predict a combination of the observed predictors in the training period. Second, we optimise the choice of the given constants to minimise the mean squared prediction error of metro service outcomes in the validation period. Finally, with the validation period data we calculate the optimal synthetic control weights based on the constants obtained in the previous stage. Both optimisation problems are formally specified in section Methodology.

For the disrupted station, Table 2 displays the optimal weights $\mathbf{C}^{a_i^*}$ of the synthetic control of each metro service outcome. These weights reflect the contribution of each normal day (\mathbf{d}_N) in the donor pool. The distribution of weights is different for each outcome. Generally, dates 16/1/2019, 11/2/2019, 13/2/2019, 21/2/2019, 05/3/2019 and 25/3/2019 tend to carry greater weights, while the remaining dates contribute less to the synthetic control.

² After matching the disruption duration with time intervals, the selected disruption occurred at the end of interval 46 for approximately 3 minutes. Such an impact can be neglected, so we set this disruption to start from interval 47.

³ If multiple disruptions occur on the same day, the synthetic control methods can only quantify their joint impacts rather than the individual impact.

Table 1. Potential predictors of metro performance.

Category	Predictors	Description
Pre-intervention outcomes (15-minutes)	Entry ridership	The number of passengers that enter the study unit before the disruption starts.
	Exit ridership	The number of passengers that exit the study unit before the disruption starts.
	Average journey time	The average journey time of passengers that enter the study unit before the disruption starts.
	Average travel speed	The average travel speed of passengers that enter the study unit before the disruption starts.
Weekday	Day of week	Dummy variable, representing whether it is on the same day of the week as the disrupted date.
Weather conditions	Temperature	Atmospheric temperature around study units, ranging from 15°C to 27°C.
	Wind speed	The wind speed around study units, ranging from 4 to 44 km/h.
	Rain status	Rain precipitation around study units, ranging from 0 to 4 mm/h.
External events	Concert	Dummy variable, representing whether there is a concert held in Hong Kong.
	Sports	Dummy variable, representing whether there is a sports match held in Hong Kong.
	Exhibition	Dummy variable, representing whether there is a large exhibition held in Hong Kong.
	Overall mega-events	Dummy variable, representing whether there are external mega-events held in Hong Kong.

Table 2. Synthetic control weights of the disrupted station (for five outcome measures).

d_N	Entry ridership	Exit ridership	Ave journey time	Ave speed	Crowding density
09/1/2019	-*	0.005	0.064	0.006	-*
16/1/2019	0.323	0.124	0.231	0.006	0.154
11/2/2019	-*	0.005	0.116	0.186	0.349
13/2/2019	0.001	0.004	0.022	0.297	0.091
21/2/2019	-*	0.229	0.024	0.098	0.406
28/2/2019	-*	-*	0.025	0.006	-*
05/3/2019	0.177	0.211	0.040	0.193	-*
13/3/2019	-*	-*	0.025	0.006	-*
14/3/2019	-*	-*	0.346	0.008	-*
20/3/2019	-*	-*	0.019	0.006	-*
25/3/2019	0.499	0.422	0.036	0.179	-*
26/3/2019	-*	-*	0.030	0.006	-*
28/3/2019	-	-	0.022	0.006	-

* “-” represents the weight is less than 1e-04.

5.2 Synthetic control performance

Figure 3 benchmarks the predictive power of (i) our synthetic control design against two naive approaches: (ii) taking the unweighted average of the historic observations in the donor pool and (iii) using the time-invariant average of pre-disruption observations (i.e., before-after comparison). We compare all three estimates to the observed data of the disrupted station. This figure shows that our weighted synthetic control can closely approximate the temporal pattern of each transport service outcome before the disruption occurrence, while the unweighted average sometimes fails. The naive

before-and-after comparison cannot capture the changes in the pre-intervention time series of the outcome variables, demonstrating the need for causal inference methods to identify the true spatiotemporal effect of disruption.

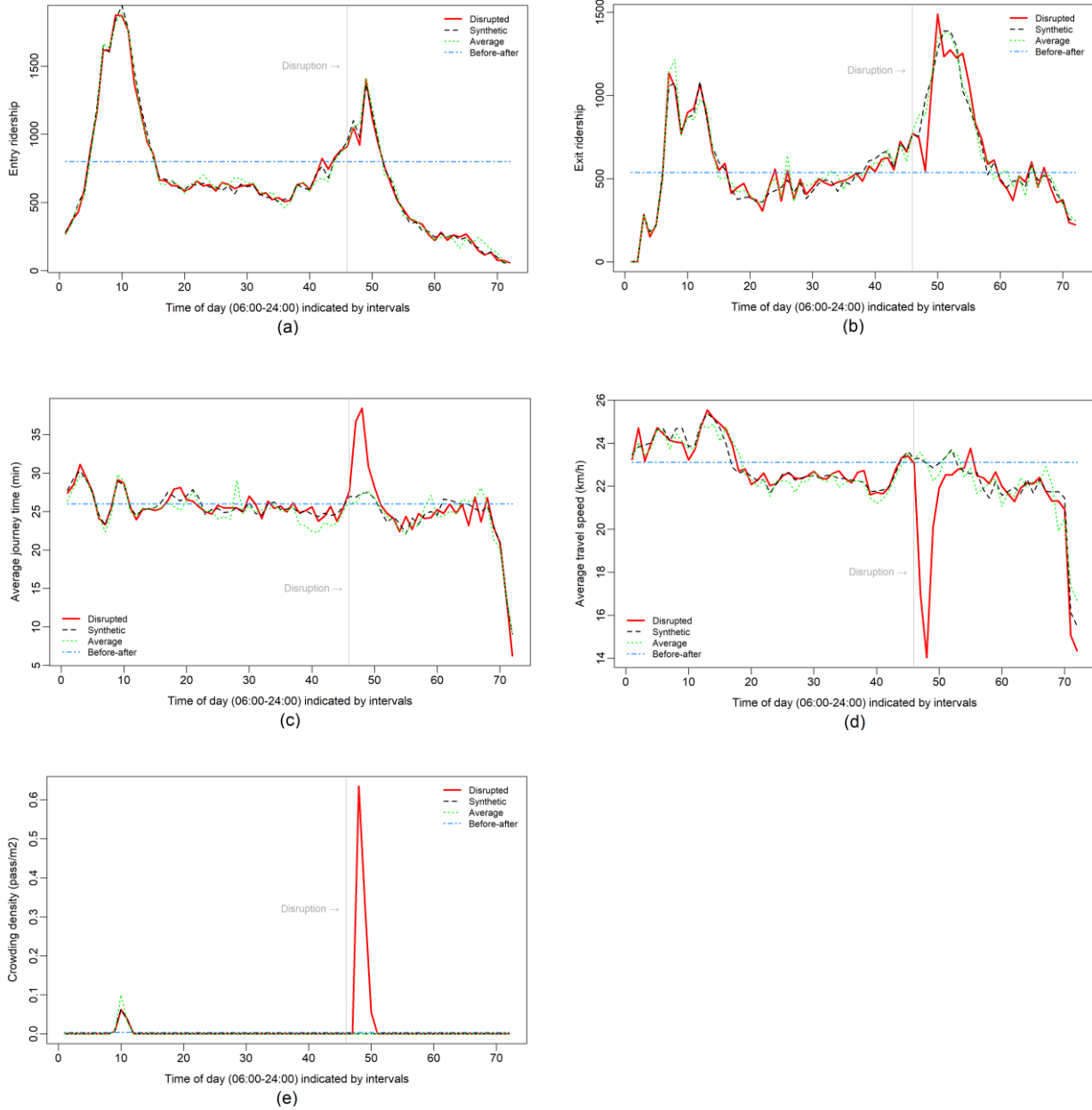


Figure 3. Results of synthetic control estimation and causal effects on the disrupted station – with comparison of other impact quantification methods.

By comparing the post-disruption patterns of the outcomes in the data to their synthetic counterfactuals, we observe the direct causal effect of the disruption at Chai Wan station. Panel (b) of Figure 3 shows that the treatment reduced the passenger flow leaving the station by around 50% during the peak of the service interruption. There is only a small impact on the entry ridership, with a decrease of just 5% during the disruption; see panel (a). This suggests that passengers at Chai Wan station had few alternative routes to avoid the delay. With regards to the average journey time, this disruption delayed the average passenger by over 11 minutes (S.E. 0.008) per trip. Therefore, the mean travel speed also

experienced a significant drop by up to 9 km/h (S.E. 0.004). The density of standing passengers inside trains grew from 0 to 0.635 person per square metre due to the accumulation of travellers while train movements were interrupted. Finally, with the resumption of train services, the impacts on exit ridership, average journey time, average speed and crowding density reached a turning point and gradually converged to the undisrupted counterfactual curve.

For the disrupted station, Table 3 reports the mean values of the average travel speed predictors before the disruption. Its columns represent (i) the data, that is, $\bar{X}_1^{a_I}$ observed on 11/3/2019, (ii) synthetic control counterfactuals $\bar{X}_0^{a_I} C^{a_I*}$ derived with the method above, (iii) the unweighted average $\frac{1}{J} \bar{X}_0^{a_I}$ of observations in the donor pool, and (iv) a single unit $\bar{X}_4^{a_I}$ from the donor pool (observed on 11/2/2019).

Table 3. Mean values of predictors for average travel speed, pre-treatment.

Predictors	Disrupted station	Synthetic control	Average control	Single control
Entry ridership	796.956	795.012	794.309	809.311
Exit ridership	532.089	532.551	527.815	537.822
Ave journey time (min)	25.945	25.954	25.960	25.475
Ave speed (km/h)	23.040	23.035	23.034	22.947
Day of week (dummy)	1	0.152	0.154	0
Temperature (°C)	19.272	20.995	22.051	18.235
Wind (km/h)	7.244	10.463	13.460	13.444
Rain (mm)	0.133	0.126	0.087	0
Mega-event (dummy)	0	0.421	0.612	0.822

The results in Table 3 illustrate that the weighted synthetic control in column 2 provides a rather accurate approximation of the values of the predictors in column 1. By contrast, the unweighted average and the single control unit both lose accuracy in the reproduction of predictors prior to the disruption. We also validate the prediction of the pre-intervention outcomes as shown in Table 4. For all metro performance measures, the weighted synthetic control outperforms the other two methods, which is in line with prior expectation based on the literature.

Table 4. Mean square prediction errors of the five outcome variables, pre-treatment.

Outcome measures	Mean square prediction error (S.E.*)		
	Synthetic control	Average control	Single control
Entry ridership	844.869 (5.435)	1874.413 (10.044)	2436.478 (229.437)
Exit ridership	1844.911 (11.674)	2356.370 (15.602)	5171.478 (249.073)
Ave journey time	0.496 (0.002)	1.632 (0.005)	2.524 (0.014)
Ave speed	0.038 (1.523e-04)	0.140 (3.017e-04)	0.270 (0.001)
Crowding density	2.177e-06 (6.256 e-07)	2.809 e-05 (1.185e-06)	1.010e-04 (4.125e-06)

*Standard errors are estimated by a bootstrapping algorithm, which randomly resamples (with replacement) the non-disrupted dates of the donor pool 1000 times.

5.3 Spillover disruption effects and propagation

In the same manner as implementing the proposed framework for the disrupted station, we obtain the weights and synthetic control estimations for other non-disrupted stations in the metro network. Adopting the same causal approach for links that did not directly receive the disruption, allows us to recover the pattern of treatment interference in the network. We use average travel speed and crowding

density as examples to illustrate how the impacts of this disruption spread to the other 48 stations spatially and temporally.

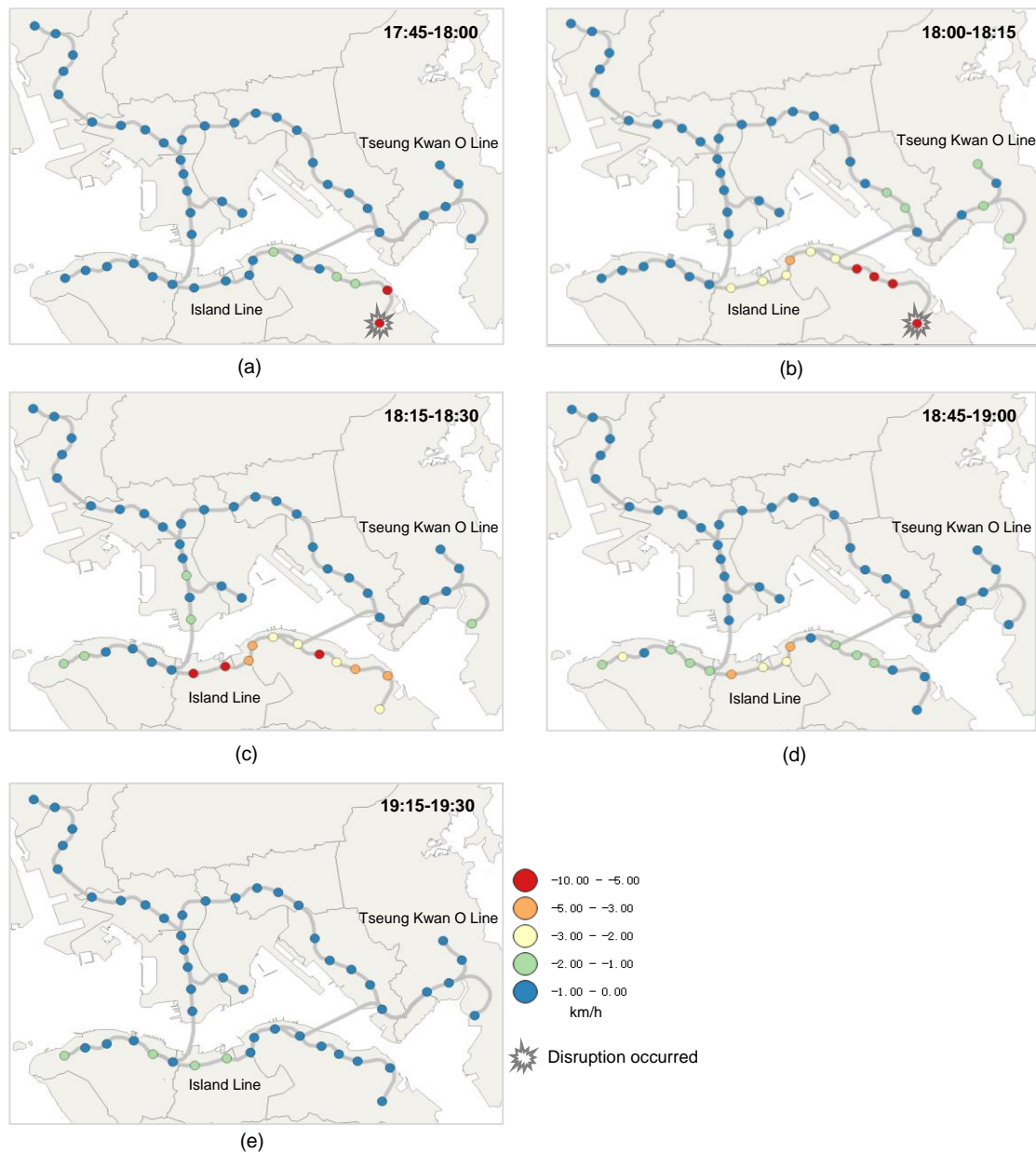


Figure 4. Spillover effects on the average travel speed at different time periods. The star symbol indicates the location of the example disruption. The nodes represent metro stations, and their colour indicates the magnitude of reduction in average travel speed due to the disruption.

Figure 4 visualises the spatial distribution of the impacts on average travel speed in five 15-minute time intervals following the disruption. The original disruption occurred at the Eastern terminus of the Island Line, affecting train traffic westbounds. In the first 15 minutes of the disruption, Figure 4(a) shows that the second station has been severely affected, and the impacts spread from the third to the seventh station. Then, during the second 15-minute interval, as shown in Figure 4(b), the disruption impacts continue to propagate along the Island Line until the tenth station, with the first four stations all in severe delay. More interestingly, stations along the connecting Tseung Kwan O Line in the Northeast are also affected, so we find evidence of a disruption spillover between lines.

The original disruption at the terminus of the Island Line disruption ends at 18:15 and train services are restored. As a consequence, in Figure 4(c) we find that disruption effects weaken at the first four stations to a moderate level. However, the remaining downstream stations of the entire Island Line, as well as the Southern part of the Tsuen Wan line, remain affected. In Figure 4(d), another 30 minutes later, the average travel speed recovers entirely around the original location of the disruption. But the delays remain very serious along the central and Western sections of the Island Line. Finally, in Figure 4(e), one hour after the disruption, the average travel speed returns to normal at most stations. See the temporal evolution of average speed plotted separately for each station in Appendix Figure A1.

Figure 5 shows how the impact on crowding spreads over time and space at each station along the Island Line. During evening peak hours, the crowding density of most stations increases right after the disruption occurred and then gradually decreases to zero within 3 hours, with considerable fluctuations. For some busy inner-city stations, the standing density reaches over 6 passengers per square metre due to the disruption, causing significant discomfort for passengers (Haywood et al., 2017; Bansal et al., 2022), even though the original disruption occurred at a remote part of the network.

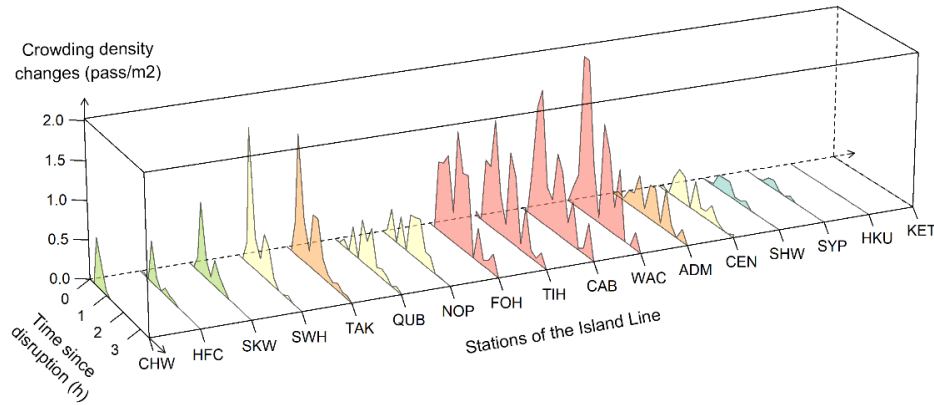


Figure 5. Spillover effects on the in-vehicle density of crowding at consecutive stations of the disrupted line. Colour coding represents crowding on board during and after the disruption (pass/m²): blue (0-0.5) green (0.5-1) yellow (1-2) orange (2-3) red (3-6).

6. Conclusions

Urban metros play an important role in the shift towards more sustainable transport and net-zero carbon emissions. However, service disruptions pose various challenges for metro systems, including delays, crowding, and a decline in passenger satisfaction and patronage. Objective measurement of disruption impacts is necessary for metro operators to understand the severity of disruptions, assess the performance of their services, and manage and mitigate future metro disruptions. Such accurate and unbiased information about the spatiotemporal effect of disruptions across the metro network is a key resource in the provision of efficient, reliable, and resilient metro services.

We propose a causal inference framework to quantify the direct and indirect (spillover) effects of disruptions on passenger demand, average journey time, average travel speed and crowding density on board. Our approach is novel in relation to the existing literature for two reasons. First, we identify the causal impact of disruptions net of confounding influences that may affect both the occurrence and impact of disruptions. Second, we extend our causal analysis to the entire network, thus exploring the propagation of disruption impacts beyond the station where the failure occurs. The proposed synthetic

control framework directly addresses interference effects, i.e., that transport service outcomes at station A affect the operating status of station B, with the aid of multi-day high-frequency smart card data. Thus, disruption impacts that spread throughout the entire network can be captured. To the best of our knowledge, this is the first study that estimates indirect disruption impacts and analyses the propagation of such effects, creating unbiased network-level empirical evidence.

The proposed method is applied in a case study of four urban lines in the Hong Kong MTR and an arbitrarily selected disruption on the Island Line. Based on the comparison of observed undisrupted metro service outcomes and counterfactual controls constructed from historic observations of a donor pool, convincing evidence has been found to support the prediction accuracy and validity of the synthetic control design.

An illustrative application of the method revealed practical insights on the process of disruption propagation in the metro network. We showed that delays may spread along the entire metro line, and even connect to other lines within the network. The propagation of spillover effects takes time, with impacts on downstream stations lagging behind those on upstream stations. Service levels may recover earlier at the disrupted station than elsewhere in the network. The unbiased measurement of this spatial and temporal lag provides important information for metro operators and could help them improve the quality of information provision and replacement service planning during disruptions.

Another interesting finding is that interchange stations with more than two metro lines are more resistant to disturbance from disruptions, especially for journey time, travel speed and crowding density. A possible explanation is that passengers at interchange stations have access to alternative routes to continue their trips, thus reducing the probability of delays and trip cancellation. Our practical lesson is that metro operators should devote increased attention to disruption mitigation at less connected stations.

In a practical setting, the research developed in this paper can be used to improve disruption management in urban mass transit systems, hopefully rendering them more resilient to unpredictable events and thus more attractive as a sustainable mode of travel for passengers.

7. Acknowledgement

The authors are grateful for the support of the Hong Kong MTR, the data provider of this research. Any opinions, findings, and conclusions or recommendations expressed in this material are those of the authors and do not necessarily reflect the views of the MTR. Prateek Bansal was supported by the Leverhulme Trust Early Career Fellowship.

8. References

- Abadie, A., 2021. Using synthetic controls: Feasibility, data requirements, and methodological aspects. *J. Econ. Lit.* 59(2), 391-425.
- Abadie, A., Diamond, A., Hainmueller, J., 2010. Synthetic control methods for comparative case studies: Estimating the effect of California's tobacco control program. *J. Am. Stat. Assoc.* 105(490), 493-505.

- Abadie, A., Gardeazabal, J., 2003. The economic costs of conflict: A case study of the Basque Country. *Am. Econ. Rev.* 93(1), 113-132.
- Adjetei-Bahun, K., Birregah, B., Châtelet, E., Planchet, J.L., 2016. A model to quantify the resilience of mass railway transportation systems. *Reliab. Eng. Syst. Saf.* 153, 1-14.
- Bansal, P., Hörcher, D., Graham, D. J., 2022. A dynamic choice model to estimate the user cost of crowding with large scale transit data. *J. Roy. Stat. Soc.: Ser. A.* 185 (2), 615–639.
- Brazil, W., White, A., Nogal, M., Caulfield, B., O'Connor, A., Morton, C., 2017. Weather and rail delays: Analysis of metropolitan rail in Dublin. *J. Transp. Geogr.* 59, 69-76.
- Cats, O., Jenelius, E., 2014. Dynamic Vulnerability Analysis of Public Transport Networks: Mitigation Effects of Real-Time Information. *Netw. Spat. Econ.* 14(3-4), 435–463.
- Chopra, S.S., Dillon, T., Bilec, M.M. Khanna, V., 2016. A network-based framework for assessing infrastructure resilience: a case study of the London metro system. *J. R. Soc. Interface.* 13(118), 20160113.
- Derrible, S., Kennedy, C., 2010. The complexity and robustness of metro networks. *Phys. A: Stat. Mech. Appl.* 389(17), 3678-3691.
- Graham, D.J., McCoy, E.J., Stephens, D.A., 2014. Quantifying causal effects of road network capacity expansions on traffic volume and density via a mixed model propensity score estimator. *J. Am. Stat. Assoc.* 109(508), 1440-1449.
- Haywood, L., Koning, M., Monchambert, G., 2017. Crowding in public transport: Who cares and why?. *Transp. Res. A: Policy Pract.* 100, 215-227.
- Hörcher, D., Graham, D. J., Anderson, R. J., 2017. Crowding cost estimation with large scale smart card and vehicle location data. *Transp. Res. B: Methodol.* 95, 105-125.
- Imbens, G.W., Rubin, D.B., 2015. Causal inference in statistics, social, and biomedical sciences. Cambridge University Press.
- Kusakabe, T., Asakura, Y., 2014. Behavioural data mining of transit smart card data: A data fusion approach. *Transp. Res. C: Emerg. Technol.* 46, 179-191.
- Malandri, C., Fonzone, A., Cats, O., 2018. Recovery time and propagation effects of passenger transport disruptions. *Phys. A: Stat. Mech. Appl.* 505, 7-17.
- Mattsson, L.G., Jenelius, E., 2015. Vulnerability and resilience of transport systems—A discussion of recent research. *Transp. Res. A: Policy Pract.* 81, 16-34.
- M'cleod, L., Vecsler, R., Shi, Y., Levitskaya, E., Kulkarni, S., Malinchik, S., Sobolevsky, S., 2017. Vulnerability of Transportation Networks: The New York City Subway System under Simultaneous Disruptive Events. *Procedia Comput. Sci.* 119, 42-50.

- Melo, P.C., Harris, N.G., Graham, D.J., Anderson, R.J., Barron, A., 2011. Determinants of delay incident occurrence in urban metros. *Transp. Res. Rec.* 2216(1), 10-18.
- Rodríguez-Núñez, E., García-Palomares, J.C., 2014. Measuring the vulnerability of public transport networks. *Transp. Geogr.* 35, 50-63.
- Rubin, D. B., 1974. Estimating causal effects of treatments in randomized and nonrandomized studies. *J. Educ. Psychol.* 66(5), 688–701.
- Rubin, G.J., Brewin, C.R., Greenberg, N., Simpson, J., Wessely, S., 2005. Psychological and behavioural reactions to the bombings in London on 7 July 2005: cross sectional survey of a representative sample of Londoners. *Bmj*, 331(7517), 606.
- Silva, R., Kang, S.M., Airolidi, E.M., 2015. Predicting traffic volumes and estimating the effects of shocks in massive transportation systems. *Proc. Natl. Acad. Sci. U.S.A.* 112(18), 5643-5648.
- Singh, R., Hörcher, D., Graham, D. J., 2023. An evaluation framework for operational interventions on urban mass public transport during a pandemic. *Sci. Rep.* 13(1), 5163.
- Sun, D.J., Guan, S., 2016. Measuring vulnerability of urban metro network from line operation perspective. *Transp. Res. A: Policy Pract.* 94, 348-359.
- Sun, D.J., Zhao, Y., Lu, Q.C., 2015. Vulnerability analysis of urban rail transit networks: A case study of Shanghai, China. *Sustainability.* 7(6), 6919-6936.
- Sun, H., Wu, J., Wu, L., Yan, X., Gao, Z., 2016. Estimating the influence of common disruptions on urban rail transit networks. *Transp. Res. A: Policy Pract.* 94, 62–75.
- Sun, L., Axhausen, K.W., Lee, D.H., Huang, X., 2013. Understanding metropolitan patterns of daily encounters. *Proc. Natl. Acad. Sci. U.S.A.* 110(34), 13774-13779.
- Sun, L., Huang, Y., Chen, Y., Yao, L., 2018. Vulnerability assessment of urban rail transit based on multi-static weighted method in Beijing, China. *Transp. Res. A: Policy Pract.* 108, 12-24.
- Wan, X., Li, Q., Yuan, J., Schonfeld, P.M., 2015. Metro passenger behaviors and their relations to metro incident involvement. *Accid. Anal. Prev.* 82, 90-100.
- Yang, Y., Liu, Y., Zhou, M., Li, F., Sun, C., 2015. Robustness assessment of urban rail transit based on complex network theory: A case study of the Beijing Subway. *Saf. Sci.* 79, 149-162.
- Yap, M., Cats, O., 2020. Predicting disruptions and their passenger delay impacts for public transport stops. *Transportation.* 48, 1703-1731.
- Yap, M., Cats, O., Törnquist Krasemann, J., van Oort, N., Hoogendoorn, S., 2022. Quantification and control of disruption propagation in multi-level public transport networks. *Int. J. Transp. Sci. Technol.* 11(1), 83-106.
- Ye, Q., Kim, H., 2019. Assessing network vulnerability of heavy rail systems with the impact of partial node failures. *Transportation*, 46(5), 1591-1614.

Zhang, D.M., Du, F., Huang, H., Zhang, F., Ayyub, B.M., Beer, M., 2018. Resiliency assessment of urban rail transit networks: Shanghai metro as an example. *Saf. Sci.* 106, 230-243.

Zhang, J., Wang, S., Wang, X., 2018. Comparison analysis on vulnerability of metro networks based on complex network. *Phys. A: Stat. Mech. Appl.* 496, 72-78.

Zhang, N., Graham, D.J., Hörcher, D., Bansal, P., 2021. A causal inference approach to measure the vulnerability of urban metro systems. *Transportation*. 48, 3269-3300.

Zhang, N., Graham, D.J., Bansal, P., Hörcher, D., 2022. Detecting metro service disruptions via large-scale vehicle location data. *Transp. Res. C: Emerg. Technol.* 144, 103880.

Zhang, X., Deng, Y., Li, Q., Skitmore, M., Zhou, Z., 2016. An incident database for improving metro safety: The case of shanghai. *Saf. Sci.* 84, 88–96.

Zhu, S., Masud, H., Xiong, C., Yang, Z., Pan, Y., Zhang, L., 2017. Travel Behavior Reactions to Transit Service Disruptions: Study of Metro SafeTrack Projects in Washington, DC. *Transp. Res. Rec.* 2649(1), 79-88.

Appendix

A.1 Source of disruption data

Based on the detection method proposed by Zhang et al. (2022), we transform the abnormal headway series that are extracted from the AVL data (train movements) into historical disruption data, which is then combined with official incident logs to build an accurate database of service disruptions. All records include the information of time and location of disruption occurrence, duration time and primary/secondary types.

Minor disruptions that lasted less than five minutes are excluded from the impact estimation. During the study period, 106 disruptions (of over 5 minutes) were observed on the four urban lines. Considering a primary disruption can spread along metro lines and lead to service interruption at other stations (secondary disruptions), the impacts of these two types of disruptions will be superimposed on each other and hence will be virtually indistinguishable. Thus, the causal effects estimated via the synthetic control framework are the integrated impacts from both the primary disruption and its corresponding secondary disruptions.

A.2 Definition and calculation of outcome measures

Entry ridership: the number of passengers who enter the given station a , on day d , during the 15-minute interval t . This measure is calculated based on the tap-in records from the smart card data.

Exit ridership: the number of passengers who exit the given station a , on day d , during the 15-minute interval t . This measure is calculated based on the tap-out records from the smart card data.

Average journey time: the average of journey time of passengers who start their trips from the given station a , on day d , during the 15-minute interval t . This measure is calculated according to the timestamp of the paired tap-in and tap-out records.

Average travel speed: the average of the speed of all trips that start from the given station a , on day d , during the 15-minute interval t . For each trip, speed is computed as travel distance divided by observed journey time. Whereas journey time is directly obtained using the smart card data, travel distance (track length) of the most probable route is derived using the shortest path algorithm. Passengers who left the system and used other transport modes to reach their final destination are not included in the computation of this metrics. If the origin station is entirely closed and no passenger can continue trips by metro, then the average speed will be zero. If the origin station is partially closed, this metrics reflects the average speed of passengers who remain in the system.

Crowding density on board: the number of standing passengers per square metre on trains that pass through the given station a , on day d , during the 15-minute interval t . The calculation of this measure follows the method proposed by Hörcher et al., (2017). By merging smart card data with train movement data, passenger to train assignments are conducted to obtain the number of passengers on board each train. Then the crowding density equals the number of passengers on board subtracting the number of seats and dividing by the available floor area.

Reference

Hörcher, D., Graham, D. J., Anderson, R. J., 2017. Crowding cost estimation with large scale smart card and vehicle location data. *Transp. Res. B: Methodol.* 95, 105-125.

Zhang, N., Graham, D.J., Bansal, P., Hörcher, D., 2022. Detecting metro service disruptions via large-scale vehicle location data. *Transp. Res. C: Emerg. Technol.* 144, 103880.